SANDIA REPORT

SAND2004-4584
Unlimited Release
Printed February 2006

Failure Analysis of Rutile Sleeves in MC3080 Lightning Arrestor Connectors

Chad S. Watson, Alice C. Kilgo, Terry L. Ernest, Sandy L. Monroe, Bruce A. Tuttle, and Walter R.Olson

Prepared by
Sandia National Laboratories
Albuquerque, New Mexico 87185 and Livermore, California 94550

Sandia is a multiprogram laboratory operated by Sandia Corporation,
a Lockheed Martin Company, for the United States Department of Energy's
National Nuclear Security Administration under Contract DE-AC04-94AL85000.

Approved for public release; further dissemination unlimited.

Issued by Sandia National Laboratories, operated for the United States Department of Energy by Sandia Corporation.

NOTICE: This report was prepared as an account of work sponsored by an agency of the United States Government. Neither the United States Government, nor any agency thereof, nor any of their employees, nor any of their contractors, subcontractors, or their employees, make any warranty, express or implied, or assume any legal liability or responsibility for the accuracy, completeness, or usefulness of any information, apparatus, product, or process disclosed, or represent that its use would not infringe privately owned rights. Reference herein to any specific commercial product, process, or service by trade name, trademark, manufacturer, or otherwise, does not necessarily constitute or imply its endorsement, recommendation, or favoring by the United States Government, any agency thereof, or any of their contractors or subcontractors. The views and opinions expressed herein do not necessarily state or reflect those of the United States Government, any agency thereof, or any of their contractors.

Printed in the United States of America. This report has been reproduced directly from the best available copy.

Available to DOE and DOE contractors from
U.S. Department of Energy
Office of Scientific and Technical Information
P.O. Box 62
Oak Ridge, TN 37831

Telephone: (865)576-8401
Facsimile: (865)576-5728
E-Mail: reports@adonis.osti.gov
Online ordering: http://www.osti.gov/bridge

Available to the public from
U.S. Department of Commerce
National Technical Information Service
5285 Port Royal Rd
Springfield, VA 22161

Telephone: (800)553-6847
Facsimile: (703)605-6900
E-Mail: orders@ntis.fedworld.gov
Online order: http://www.ntis.gov/help/ordermethods.asp?loc=7-4-0#online

SAND2004-4584
Unlimited Release
Printed February 2006

Failure Analysis of Rutile Sleeves in MC3080 Lightning Arrestor Connectors

Chad S. Watson
Ceramics and Glass Processing

Alice C. Kilgo
Materials Characterization

Terry L. Ernest
Passive Devices/Interconnects

Sandy L. Monroe
Materials Reliability

Bruce A. Tuttle
Microsystems Materials and Mechanical Behavior

Walter R. Olson
Microsystems Materials and Mechanical Behavior Department

Sandia National Laboratories
P.O. Box 5800
Albuquerque, NM 87185

ABSTRACT

The purpose of this SAND Report is to document efforts in the extraction and failure analyses of sleeve-style Lightning Arrestor Connectors (LACs). Several MC3080 and MC3079 LACs were recovered from the field and tested as part of the Enhanced Surveillance Campaign. A portion of these LACs failed retesting. Terry Ernest (01733), the LAC Component Engineer, provided eleven MC3080 LACs for evaluation where four of the LACs failed IR/DCW and one failed FRB requirements. The extraction of rutile sleeves from failed LACs was required to determine the source of failure. Rutile sleeves associated with connector function failures were examined for cracks, debris as

well as any other anomalies which could have caused the LAC to not function properly. Sleeves that failed FRB or that experienced high FRB exhibited high symmetry, smooth surface, long-flow amicon, and slightly over-sized inside diameter. LACs that failed DCW or IR requirements had rutile sleeves that exhibited breakdown tracks.

ACKNOWLEDGEMENTS

Technical contributions from Dick Grant, Tony Ohlhausen and Regina Simpson are gratefully acknowledged. The authors would like to acknowledge insightful discussions with Bob Anderson, David Cain, Gordon Pike, Dave Tallant and Raj Tandon. Sandia is a multiprogram laboratory operated by Sandia Corporation, a Lockheed Martin Company, for the United States Department of Energy's National Nuclear Security Administration under Contract DE-ACO4-94-AL85000.

Intentionally Left Blank

TABLE OF CONTENTS

FIGURES

TABLES

1. INTRODUCTION

This SAND Report documents efforts in the extraction and failure analyses of sleeve-style Lightning Arrestor Connectors (LACs). As part of the Enhanced Surveillance Campaign, MC3080 and MC3079 LACs were recovered from the field and retested. A portion of these LACs failed fast rise time voltage breakdown (FRB), direct-current voltage withstanding (DCW) and/or insulation resistance (IR) testing requirements.[1] The extraction and failure analysis of rutile sleeves from failed LACs was performed to ascertain failure mechanisms. The focus of this investigation was limited to the MC3080 LAC, but the results extend to other sleeve-style LACs. MC3080 LAC testing requirements and conditions are listed in Table I. The MC3080 LAC is in the W80-0,1 and the B61-3,4,7,10, 11 weapons systems.

2. BACKGROUND

LACs provide electrical signals to the weapon interior while also protecting sensitive components from abnormal electrical energy by diverting current to the weapon case during abnormal voltage conditions (lightning). Under a high voltage condition, an arc initiates from the electrical contact (pin) to the stainless steel web which functions as a ground plane. The arc initiating voltage is lowered with the use of a dielectric material in the air gap between the contact and the stainless steel web. In the case of early sleeve-style LACs (MC3080, MC3079, MC2995, etc), rutile (TiO_2) was used as the dielectric in the form of solid sleeves. Cracks in the rutile sleeve, sleeve symmetry, and/or metallic contamination may cause a LAC to not meet electrical requirements.

FRB, IR and DCW are product acceptance tests. The FRB requirement ensures that downstream systems are protected from high voltages associated with lightning strikes (Nuclear Safety issue). The DCW requirement tests for leakage current in the LAC between all contacts and the web. Appreciable leakage current can be due to metallic contamination in the breakdown chamber as well as from conductive breakdown tracks in the sleeve. A current path to ground is available if a lightning strike were to occur; however, signals into and out of the LAC may be compromised by this low impedance path (Reliability issue). The IR requirement evaluates the resistivity of individual contacts with respect to other contacts and the shell. Any contact that does not meet the FRB/IR/DCW requirements will result in the LAC being rejected for WR use.

Table 1. MC3080 Testing Requirements

Test	Requirements	Conditions
Fast Rise Time Voltage Breakdown (FRB)	Breakdown must occur ≤ 2000 V	10 kV/μs rise time to breakdown
DC Voltage Withstanding (DCW)	Leakage current < 1 mA	500 V/s rise time and held at 510 VDC for 120 s between all contacts and shell
Insulation Resistance (IR)	IR > 500 MΩ	500 V/s rise time and held at 510 VDC for 2 s with all remaining contacts in common with the shell

3. RUTILE SLEEVE EXTRACTION

A cross-section of an MC3080 LAC is shown in Fig. 1 and a schematic of the rutile sleeve configuration is shown in Fig. 2. The piece parts of interest are the rutile sleeves which are embedded within the interior of the LAC. Because the rutile sleeves are intimately integrated within the LAC assembly, several steps were required for extraction while all the time keeping the relatively fragile sleeves in their original condition. Otherwise, damage induced during the extraction process can complicate failure analysis.

3.1 EXTRACTION PROCEDURE

After several iterations, a process to extract rutile sleeves from LACs was established. The steps required for rutile sleeve extraction are outlined below. A majority of these steps were adapted from a Laboratory Test Method entitled, "Procedure for Performing

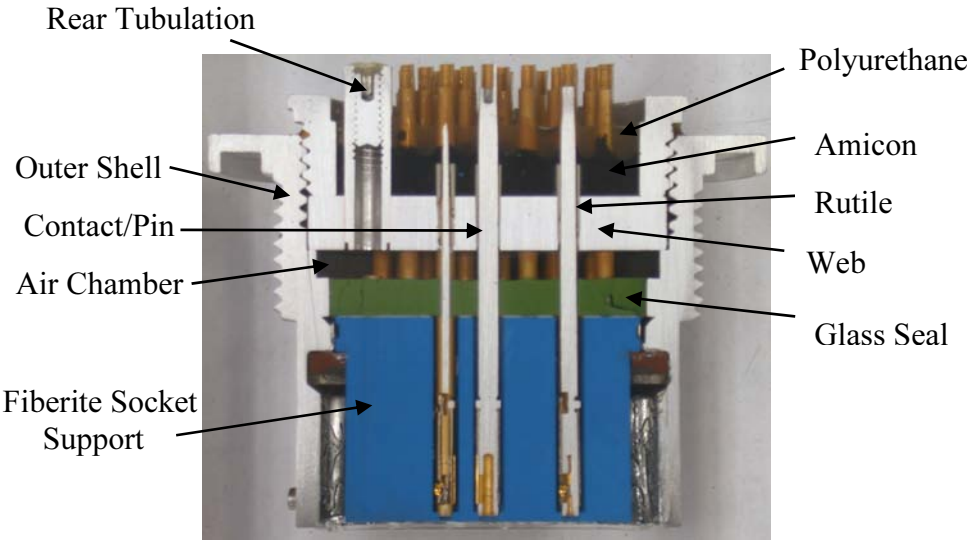

Fig. 1 Cross-section of an MC3080 LAC. The diameter of the stainless steel web is 31.75 mm.

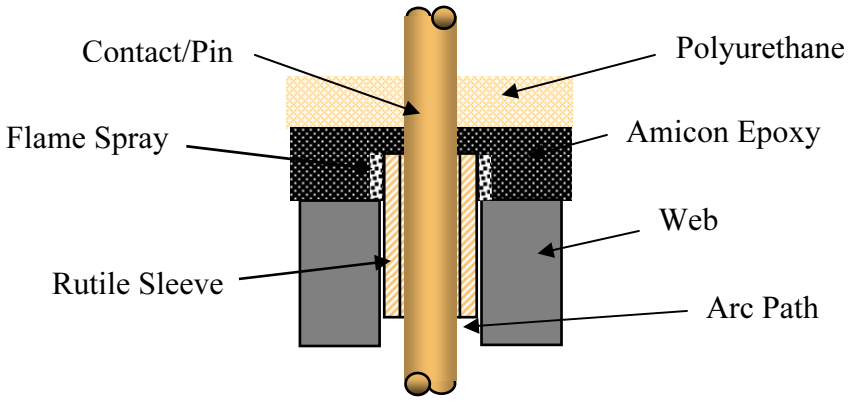

Fig. 2 Schematic of the rutile sleeve configuration in a LAC.

Defect Analysis on Sleeve Style Lightning Arrestor Connectors (LACs)," that was authored by G.W. Franti.[2]

i. The polyurethane cap was sectioned ~41.7 mm from the base of the LAC. Cuts were made directly above the rear tubulation. The purpose is to gain access to the rear tubulation for removal of the setscrew and to backfill the air chamber with epoxy. The feed rate and rpm was tightly controlled in order to minimize vibration and possible extraneous bending stresses on pins which could damage the rutile sleeves. A Struers Secotom-10 saw with a resin bonded diamond blade running at 2700 rpm and a feed rate of 0.010 mm/s was used to section the polyurethane cap. The part was clamped to prevent movement during cutting. Water was used at all times during the sectioning operation to prevent overheating of the part and the blade.

ii. Using dental tools, excess polyurethane was removed from the recess in the tubulation to expose the top of the setscrew. Using heat resistant gloves and a vice to hold the LAC, a minimum flame on a propane torch was aimed on the epoxy around the screw until it began to bubble and most of it had evaporated. The setscrew was removed quickly with an Allen wrench before the epoxy re-hardened. Once the setscrew was removed, the flame was focused at the rear tubulation (50-75 mm away from the part) and the remaining epoxy was vaporized without leaving any residue. Care was taken to ensure that no debris contaminated the cavity region and to ensure that the LAC did not overheat.

iii. The cavity region was backfilled with epoxy to stabilize the pins during subsequent slicing operations. Scotch tape was placed around the remaining polyurethane cap to create a pseudo-cup to hold the epoxy. The cavity was backfilled with a two part epoxy (Epofix, Struers, Inc.) requiring 10 parts by weight of epoxy resin to 1.2 parts by weight of hardener. 50 gm of epoxy resin was mixed with 6 gm of hardener and the epoxy was stirred for approximately 2 min to ensure a homogeneous mixture. After mixing, the epoxy was placed in a vacuum chamber to remove the air introduced during mixing (~5-10 min). A small amount (~30 ml) of the epoxy was poured into the cup created on the remaining polyurethane cap and the LAC assembly was placed in the vacuum chamber. Air in the chamber was evacuated while the epoxy flowed into the chamber, which takes several minutes because there is only one hole for both the air to escape and the epoxy to flow in to. If necessary, more epoxy was poured in the cup and the evacuation process was repeated until no air came out of the hole and no epoxy flowed into the cavity. The epoxy was cured overnight at room temperature. To prevent the epoxy from overheating during curing, the LAC was kept in a well ventilated area and placed on a large metal block to act as a heat sink.

iv. Unnecessary epoxy and polyurethane was removed from the LAC by sectioning ~37.3 mm from the base. A Struers Secotom-10 saw with a resin bonded diamond blade running at 2700 rpm and a feed rate of 0.010 mm/s was used to

slice the excess epoxy and polyurethane cap. The LAC was clamped to prevent movement during cutting. Water was used at all times during the sectioning operation to prevent overheating of the part and the blade.

v. The LAC was sectioned through the green glass ~21.1 mm from the base. The feed rate and rpm was tightly controlled in order to minimize vibration and possible extraneous bending moments on pins which could damage the rutile sleeves. With the part securely clamped, a Struers Secotom-10 saw was used to section the LAC. A low concentration metal bonded diamond blade at a feed rate of 0.10 mm/s and a blade speed of 2700 rpm was used to make the section. Water was used to keep the part and blade from overheating during sectioning.

vi. The LAC was ground and polished to the glass/epoxy interface. Grinding was performed by hand with SiC paper and water as a lubricant. Wheel speed was set to about 300 rpm. With 320 grit SiC paper, the LAC was ground until a flat surface was achieved. Once achieved, 600 grit SiC paper was used until all previous grinding damage was removed and only 600 grit scratches remained. The ground surface was hand polished with 15 μm polycrystalline diamond paste and Buehler Metadi Extender on Gold Label nylon until all 600 grit scratches were removed. The 15 μm polishing step was repeated if necessary, otherwise, 6 μm diamond paste and Buehler Metadi Extender on Gold Label nylon was used to remove all 15 μm scratches. Finally, 1 μm diamond paste on Buehler Mastertex cloth with Buehler Metadi Extender was used until all 6 μm scratches were removed and a mirror finish was achieved. The wheel speed was set to about 150 rpm for the polishing procedures. The part was inspected at this point for any debris that may be in the cavity.

vii. After the initial inspection, the LAC was ground and polished to the epoxy-stainless steel web interface. Grinding was performed by hand with SiC paper and water as a lubricant at a wheel speed of 300 rpm. 120 grit SiC paper was initially used followed by 600 grit until the stainless steel web was reached. At which point, the LAC was polished according to the procedures outlined in Step vi. The sleeves were inspected for cracks, symmetry, contamination and surface morphology. Any anomalies were noted and representative photomicrographs were taken for documentation. Pins that failed FRB/BCW/IR requirements received additional scrutiny.

viii. The outer shell was removed by making two cuts 180° apart. Cuts were sufficient in depth so that the outer shell was easily removed, but not too deep as to interact with pins. A Struers Secotom-10 saw with a SiC blade with a blade speed of 4500 rpm and a feed rate of 0.150 mm/s was used to make the cuts. For this procedure, the remaining LAC assembly was clamped with the polished side up. The first cut was made into the area where the setscrew was removed (Fig. 3). The LAC assembly was turned polished side down and cut in the same area, but further into the shell on the back side. The LAC was rotated ~180° and the cutting process was repeated. Care was taken to avoid cutting too far into the web

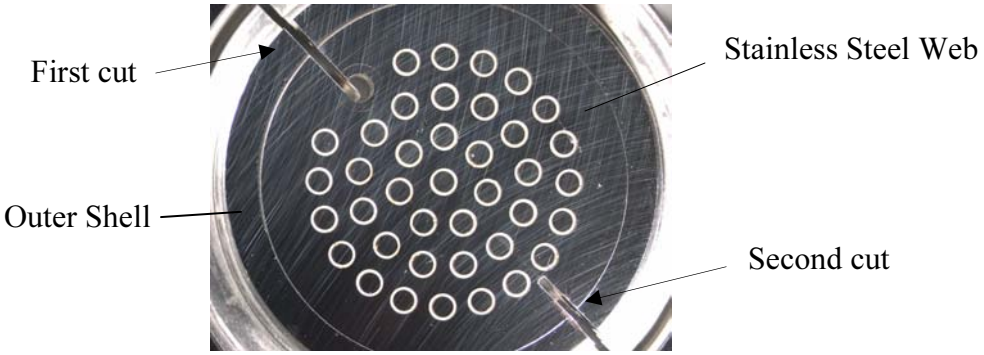

Fig. 3 Location of cuts needed to remove the outer shell. The diameter of the stainless steel web is 31.75 mm.

from the web/shell interface. The outer shell was removed by placing a flathead screwdriver into one of the cuts and prying apart the outer shell. This procedure was necessary to minimize the amount of time the LAC assembly is in the aqua regia solution used to dissolve the stainless steel.

ix. In order to examine the entire length of the sleeves in question, the stainless steel webbing was dissolved in an aqua regia solution. A solution consisting of 6 parts deionized H_2O, 3 parts highly concentrated HCl and 1 part by volume highly concentrated HNO_3 was typically used. Different concentrations of the aqua regia solution may be used to accelerate or slow the dissolution process. Once the appropriate concentration and volume was attained, the remaining LAC assembly was placed in the aqua regia solution. Either a Teflon or Pyrex beaker was used to contain the aqua regia solution and LAC during dissolution. The time required for complete dissolution of the stainless steel was typically 2-3 days. The reactivity of the solution was typically spent after one day; as a result, the LAC assembly would be placed in new aqua regia solution to continue the dissolution process at an acceptable rate. An example of a LAC assembly undergoing dissolution is shown in Fig. 4. After the web and pins were dissolved, the remaining LAC assembly was rinsed in water and air dried. The remaining LAC assembly consists of rutile sleeves protruding from the amicon (Fig. 5).

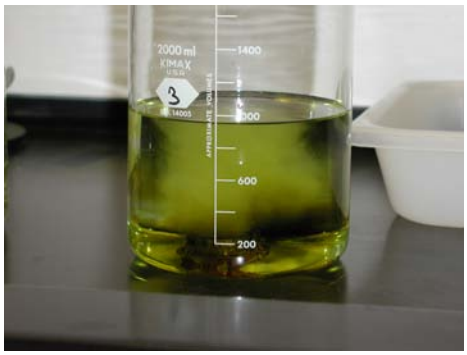

Fig. 4 Example of the LAC assembly undergoing the acid dissolution process.

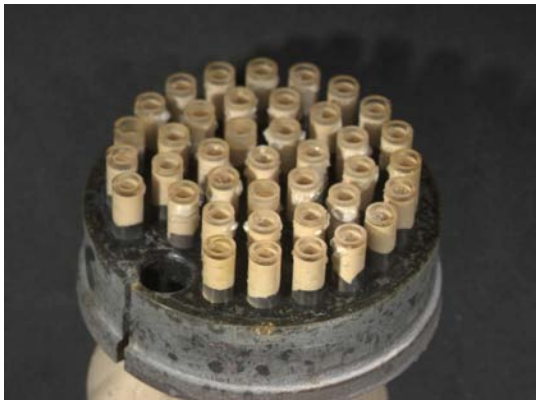

Fig. 5 LAC assembly after acid dissolution. Sleeve outside diameters are ~2.25 mm.

x. Additional characterization of failed sleeves required the removal of the sleeves from the amicon. A slow speed saw with a diamond blade was used to carefully cut into the amicon around the sleeve of interest. The blade speed was kept as low as possible and measures were taken to avoid bumping or hitting the sleeves, as they are very fragile. Sleeves removed from the remaining LAC assembly were traced back to their original location in the part. At this point, there was still a small amount of resin left on the sleeve. For the epoxy dissolution process, Allied High Techs Epoxy Dissolver was used which required a temperature of ~75°C for complete dissolution. During the epoxy dissolution process sleeves had a tendency to fracture; as a result, less severe techniques to remove the remaining amicon are being pursued.

Several extraction iterations were necessary to establish a process that resulted in the least damage to the sleeves. Although the process outlined above enables extraction, damage to the sleeves due to sawing and grinding operations as well as from chemical exposures and thermal excursions cannot be completely ruled out. Consequently, prudence must be exercised when interpreting the results.

4. RUTLE SLEEVE EXTRACTION PROVE-IN

Eleven MC3080 LACs were provided for extraction prove-in and failure analysis activities (Table II). Of the 11, a total of 5 were considered failures based on FRB, DCW and/or IR requirements. The serial numbers with an asterisk (Table II) are associated with LACs that were disassembled. A portion of the LACs that passed Enhanced Surveillance retesting were disassembled to prove-in the rutile sleeve extraction process. Attempts to prove-in the disassembly process were made on MC3080 LACs with serial numbers 105250-K81, 902045-D79 and 805036-F78.

Table 2. Summary of MC3080 LAC Retesting Data

Serial Number	Pins	100 V IR	DCW 500V	500 V IR	FRB
105250-K81*	All	Pass	Pass	Pass	Pass
902045-D79*	All	Pass	Pass	Pass	Pass
805036-F78*	All	Pass	Pass	Pass	Pass
102160-D81	All	Pass	Pass	Pass	Pass
904050-F79	All	Pass	Pass	Pass	Pass
80308049	All	Pass	Pass	Pass	Pass
102173-D81	K	2	Fail[a]	Pass	Pass
	T	Pass	Fail[a]	293	Pass
	U	Pass	Fail[a]	121	Pass
	V	Pass	Fail[a]	88	Pass
102174-D81	J	Pass	Fail[a]	0	Pass
102178-D81*	A	Pass	Fail[a]	0	Pass
	W	Pass	Fail[a]	421	Pass
105251-K81*	B	Pass	Fail[a]	1	Pass
902093-D79*	m	Pass	Pass[a]	Pass	2199 V

[a]DCW results are not isolated to one pin but are associated with all pins in the LAC.

4.1 LAC SN105250-K81

The first attempt to prove-in the disassembly process was on LAC SN105250-K81. The air chamber was backfilled with epoxy and cross-sectioned at the glass/air chamber-epoxy interface. The remaining assembly was placed in a solution of diluted agua regia to dissolve the stainless steel casing and webbing. Several iterations of time immersed in solution and aqua regia concentrations were attempted. Not all of the stainless steel was dissolved and several of the rutile sleeves cracked, most likely from the extra processing steps used to dissolve the stainless steel. Because the extraction conditions were less than ideal, no attempt to characterize the rutile sleeves was made. Based on this process prove-in attempt, modifications to the disassembly process were made on the next LAC (SN902045-D79).

4.2 LAC SN902045-D79

LAC SN902045-D79 was cross-sectioned at the glass/epoxy interface and polished for initial inspection (1st Polish). At this point, any debris in the air chamber that is trapped by the back-filled epoxy is noted. No trapped debris was observed. The LAC was polished to the web/epoxy interface for closer inspection of the rutile sleeves (2nd Polish). The 2nd polish is conducive to the use of vicinal lighting which helps delineate cracks. Any anomalous pin/sleeve symmetry (perfectly symmetric), cracked sleeves or contamination were noted during the inspection after the 1st and 2nd polish. All sleeves and pins appeared to be asymmetrically aligned within the slots in the stainless steel webbing. The ends of some of the sleeves had what appeared to be metallic contamination. The concentration of the silver-looking contamination ranged from a few specs (Fig. 6a) to a light coating (Fig. 6b). This metallic-looking contamination could be from handling during the assembly of the LAC. In particular, if tweezers were used to place the sleeves in the appropriate slots, residual metal could have easily been transferred to the sleeves. This contamination did not appear to influence FRB/IR/DCW results.

Cracks were observed on the ends of two sleeves after the 1st polish (Fig. 7), and are located in the rutile sleeve that is in contact with the stainless steel webbing. After polishing to the web/epoxy interface (2nd polish), cracks that were not observed after the initial inspection were located (Fig. 8). These cracks may have either been created during the subsequent polish or they may have been too subtle to observe without proper vicinal lighting. As with the cracks shown in Fig. 7, the cracks in Fig. 8 are located at the ends of the rutile sleeve in contact with the stainless steel webbing. A potential source for cracking is thermal cycling during LAC manufacture and/or while in the field which resulted in the development of stresses high enough for crack initiation. However, if these cracks were present in the LAC prior to disassembly, they did not affect FRB/IR/DCW results. Another potential source of cracking is from handling during disassembly.

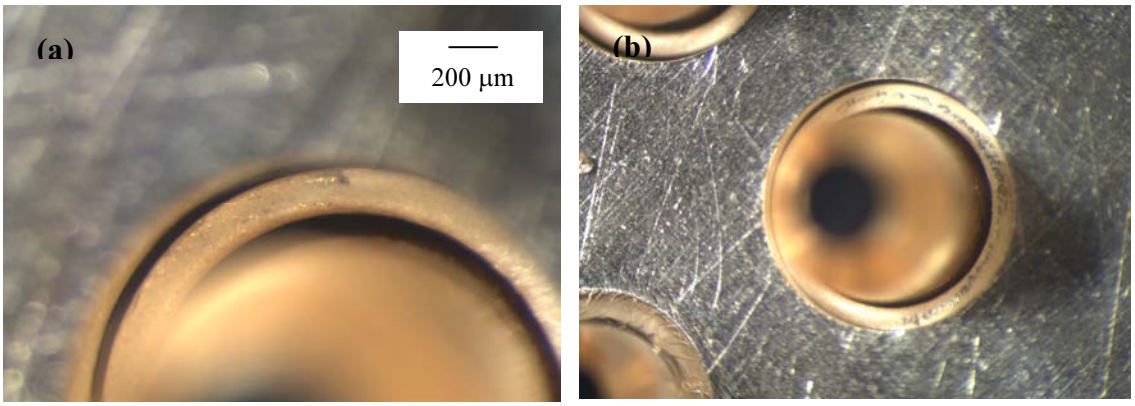

Fig. 6 Representative images of metallic-looking contamination on the ends of sleeves associated with (a) Sleeve R and (b) Sleeve U.

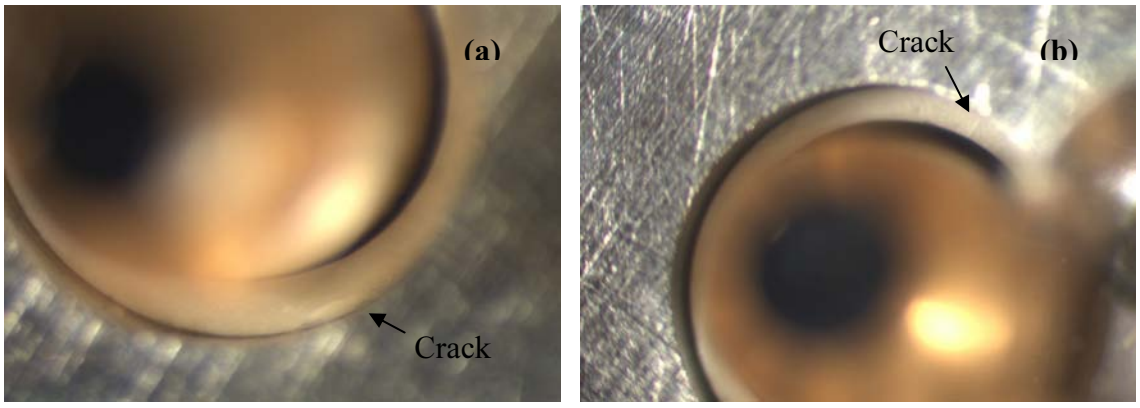

Fig. 7 Cracks observed in sleeves after the 1st polish: (a) Sleeve A and (b) Sleeve a. Wall thickness of the rutile sleeves is approximately 225 μm.

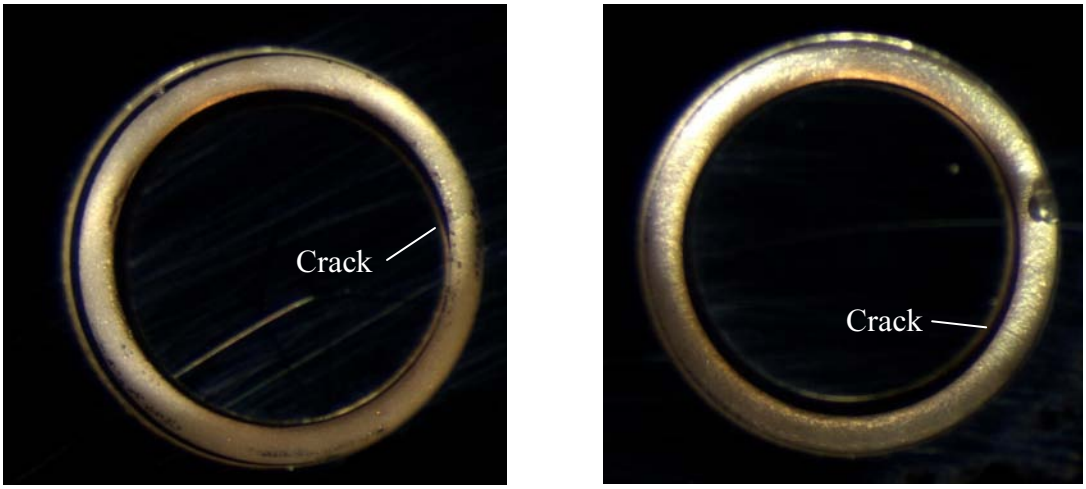

Fig. 8 Cracks observed in sleeves after the 2nd polish: (a) Sleeve b and (b) Sleeve k. Wall thickness of the rutile sleeves is approximately 225 μm.

After the 2nd polish, the outer shell casing was removed to limit the amount of time the rutile sleeves were exposed to the aqua regia solution. Once removed, the remaining assembly was placed in aqua regia until all of the stainless steel was dissolved. After complete dissolution, a Jeweler's saw and a Dremel tool were used to isolate sleeves of interest. Both methods resulted in severe damage and alternate methods to isolate sleeves were used in subsequent disassemblies.

4.3 LAC SN805036-F78

After the 1st polish, a large metal flake was observed between Pins L and M (Fig. 9). The flake was introduced during the removal of the set screw in the rear tubulation. The set screw could not be removed using an Allen wrench; as a result, a hole was drilled through the rear tubulation. The flake is scrap from the drilling process. If metallic

Fig. 9 The metal flake is an artifact of drilling into the rear tubulation to gain access to the air gap between the glass seal and the stainless steel webbing. The diameter of the web hole is approximately 2.32 mm.

debris were present in the air chamber and in contact with the web and pins, the LAC would fail DCW and pins in contact with the debris would fail IR. One apparent affect of metallic debris in the air chamber would be variability in which pin failed IR, because it could easily be dislodged to another region in the air chamber. Subsequent removal of the setscrew was accomplished by carefully heating the rear tubulation with a blowtorch and quickly unscrewing the set screw with an Allen wrench. The setscrew cannot be removed with an Allen wrench at room temperature because it is "glued" into place.

All pins/sleeves exhibited asymmetric alignment. No cracks were observed after the 1st polish. The 2nd polish revealed that some sleeve ends contained metallic-looking contamination (Fig 10). In addition, a majority of the rutile sleeves in LAC SN805036-F78 exhibited a higher frequency of edge chipping and higher surface roughness than sleeves from the other LACs that were examined as part of this study. Representative images of sleeves with extensive surface damage are shown in Fig. 11. Even though there is variability in chip out, surface roughness and metallic contamination, all of the pins in LAC SN805036-F78 passed FRB/IR/DCW. Only one sleeve (Sleeve W) had a crack (Fig 11a).

After the 2nd polish, the outer shell casing was removed to limit the amount of time the rutile sleeves were exposed to the aqua regia solution. After acid dissolution of the pins and webbing, representative images of the sleeves protruding from the amicon were made (Fig 12). The amicon wicked up on all of the rutile sleeves. Even though there is variability in the amicon height, all of the pins passed FRB/IR/DCW. The amicon height variability is typical of all the sleeves examined from the LACs and is a result of processing variables.

A fixture was designed which enabled the protruding sleeves to be captured and traced back to their position in the LAC. Unfortunately, during the epoxy dissolution process many of the sleeves fractured. This may have been the result of the elevated temperature used to dissolve the epoxy resulting in thermal stresses and ultimately fractured sleeves.

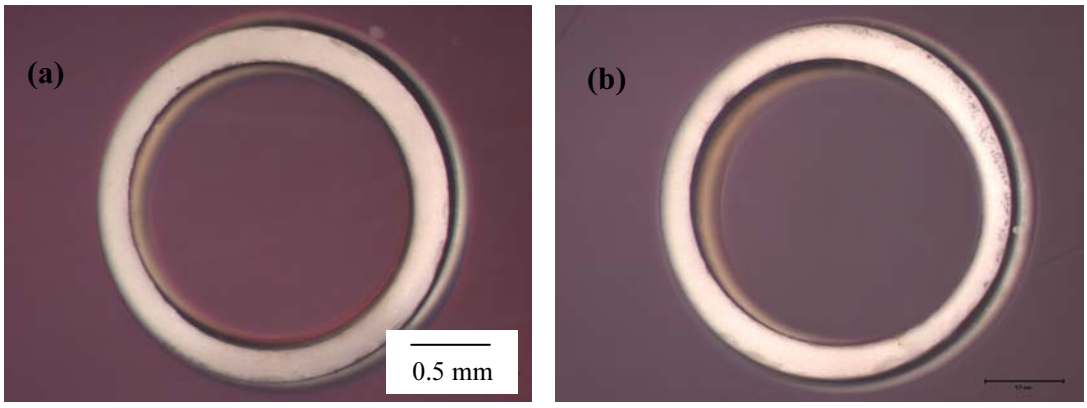

Fig. 10 Representative images of metallic-looking contamination on (a) Sleeve L and (b) Sleeve H .

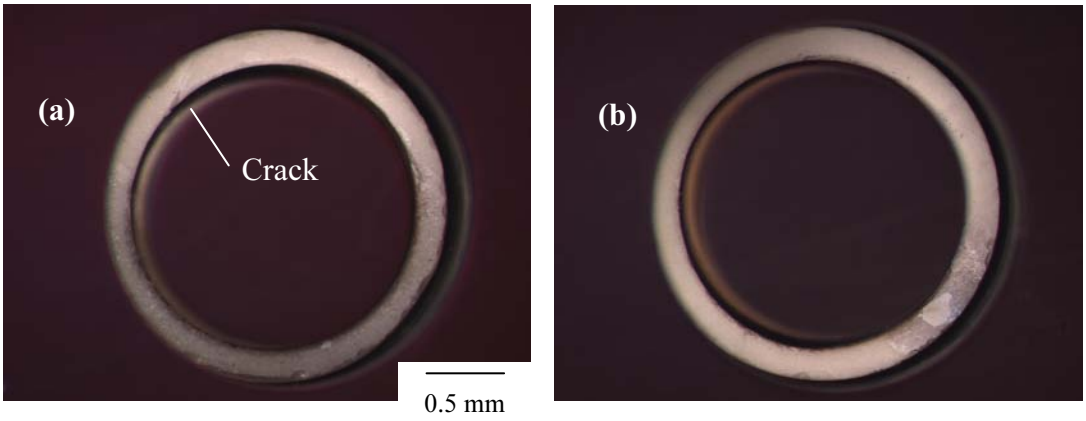

Fig. 11 Example of a sleeves (a) W and (b) B with surface damage. Sleeve W also appears to be cracked.

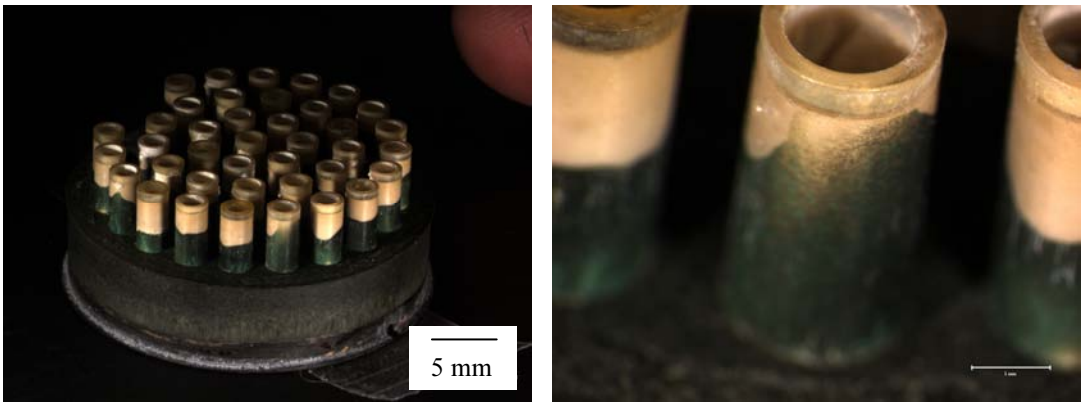

Fig. 12 Representative images showing rutile sleeves protruding from the amicon as well as the degree in which amicon wicked up the rutile sleeves.

These three prove-in iterations have enabled us to extract sleeves without causing extensive damage prior to the epoxy dissolution process. Ultimately, it was decided to cut around the sleeves of interested and then dissolve the surrounding amicon. This was found to be the best technique to keep the sleeves intact during the epoxy dissolution process.

5. FAILURE ANALYSIS

5.1 LAC SN902093-D79

Pin m from LAC 902093-D79 failed FRB at a breakdown voltage of 2199 V. To pass FRB, a breakdown voltage of 2000 V or less must be achieved. After the initial cross-section no obvious anomalies were observed with respect to Pin m. It has been hypothesized that FRB failures are the result of symmetrical alignment of the pin within the sleeve and the sleeve within the web hole.[3] Nearly symmetrical alignment of Pin and

Sleeve m was observed (Fig. 13). The asymmetry of the Sleeve m assembly was not nearly as extensive as seen in most sleeve/pin/web assemblies that were examined as a part of this study.

The stainless steel was dissolved in diluted aqua regia for a closer examination of Sleeve m and to observe other characteristics of this LAC. Amicon height was noted to reach the ends of Sleeves T, S, R, P, M, L, K, G, a, e, k, and n. Representative images of amicon height are shown in Fig 14. The amicon height on Sleeve m nearly reached the end of the sleeve (Fig. 15a). Sleeve m remained intact during isolation and epoxy dissolution (Fig. 15b).

Previous work has shown that long-flow amicon, very smooth sleeves (no chipping and negligible surface roughness) with the inside diameter of the sleeve slightly larger than the pin can result in FRB failures.[4] The amicon height on Sleeve m extended very near the sleeve end (Fig. 15a). Sleeve m also exhibited a smooth surface finish, a slightly oversized inside diameter and near-symmetrical alignment; all of which are consistent with sleeves that are more susceptible to FRB failures.

Fig. 13 For Pin m, both the pin and sleeve are nearly symmetrically aligned within the stainless steel web slot. This pin failed FRB at 2199 V. Wall thickness of the rutile sleeves is approximately 225 μm.

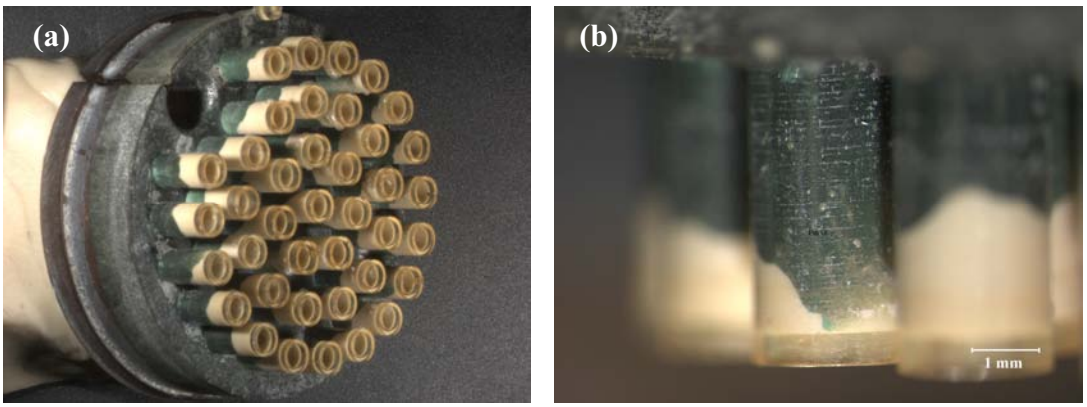

Fig. 14 (a) LAC assembly after epoxy dissolution (note amicon height) and (b) a representative image of amicon that reached the end of the sleeve (Sleeve G). Sleeve outside diameters are ~2.25 mm.

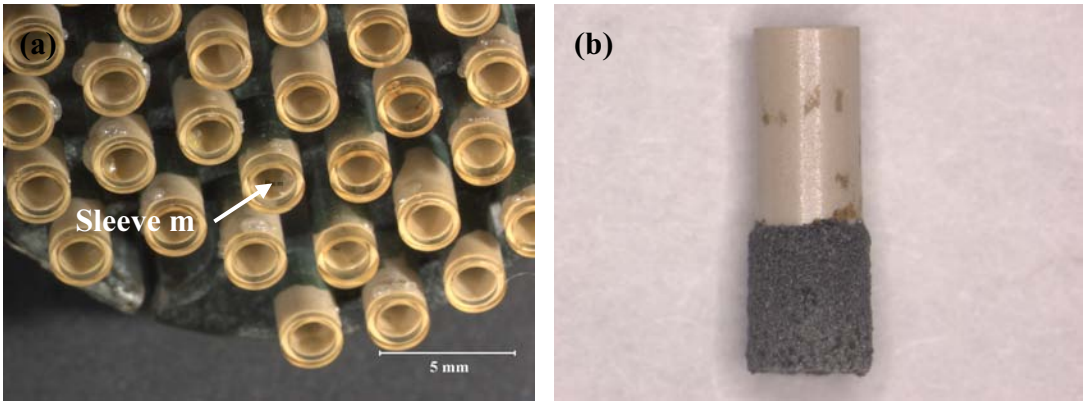

Fig. 15 Photomicrographs documenting (a) amicon height on Sleeve m and (b) the intact sleeve after epoxy dissolution. Note the flame sprayed metal on the sleeve. Sleeve outside diameters are ~2.25 mm.

5.2 LAC SN102178-D81

Pin A and W failed IR. This pin, as well as all of the pins, were tested for FRB prior to IR and DCW. Pin A passed FRB at 1028 V and Pin W passed at 1237 V. Incidentally, 1028 V was the lowest FRB of all the pins for this LAC where the average was 1200 V. After FRB, Pins A and W were tested for IR at 100V and passed. Then the LAC was tested for DCW and broke down after 1 s at a voltage of 391 V. Subsequent IR at 510 V registered failures for Pin A (current limit of instrumentation was reached) and Pin W (461 MΩ).

After the 1st polish, a chunk of rutile was observed in the air chamber (Fig. 16). This piece of rutile sleeve is not associated with any of the sleeves in this LAC. All of the sleeves were intact as observed from sleeve ends. Of the six LACs that were disassembled, this is the only LAC that contained a foreign material in the air chamber that was not inadvertently introduced during the disassembly process.

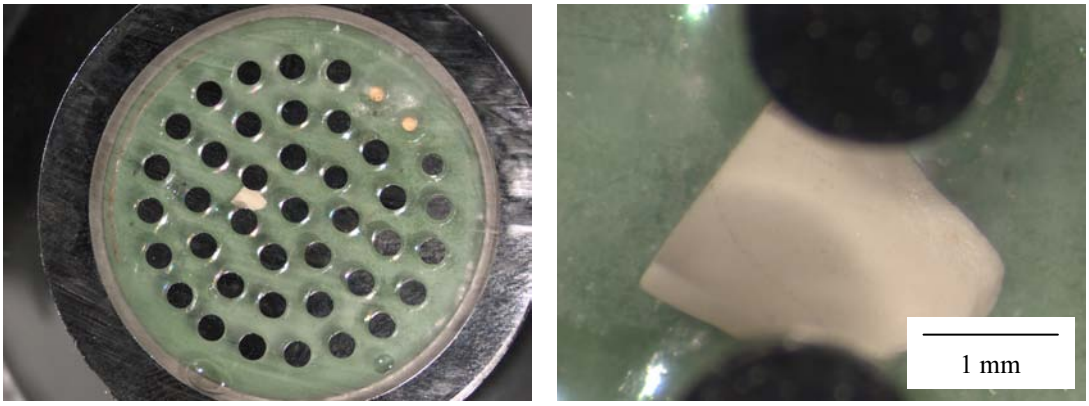

Fig. 16 A piece of rutile was found in the air chamber after the 1st cross-section.

All pins and sleeves appeared to be asymmetrically aligned and slight metallic-looking residue was observed on the ends of some sleeves. Cracks were located in Pin A (Fig. 17a) after the 1st polish and Pins E (Fig. 17b), F (Fig. 17c), and n after the 2nd polish. As noted before, cracks tend to be located within the sleeve that is in contact with the web and/or pin. These cracks are typically very fine and very shallow.

Overall the amicon height was slightly above the amicon base (Fig 18). Sleeve X was the only sleeve to have amicon at the sleeve end. Examination of the sleeves after the acid dissolution process revealed nothing unusual with Sleeve W; however, the cracks in Sleeve A shown in Fig. 17a were relocated. What appeared to be two cracks in Fig. 17a are actually the ends of one crack (Fig. 19). The crack is outlined with a red dotted line in Fig. 19 to help visualize the crack trajectory. Sleeve A fractured during the epoxy dissolution process. The crack in Sleeve A caused the cracked portion of the sleeve to chip out (Fig. 20). A blackish mark is observed on the crack surface (Fig. 20). The black mark is indicative of an electric breakdown track. During electric breakdown, very high temperatures can be reached, resulting in localized melting and possibly vaporization.

Scanning electron microscopy was utilized to characterize the morphology of the ceramic in and around the black mark (Fig. 21). Photomicrographs within the black mark show an area with a fused character and less porosity than the surrounding, undamaged

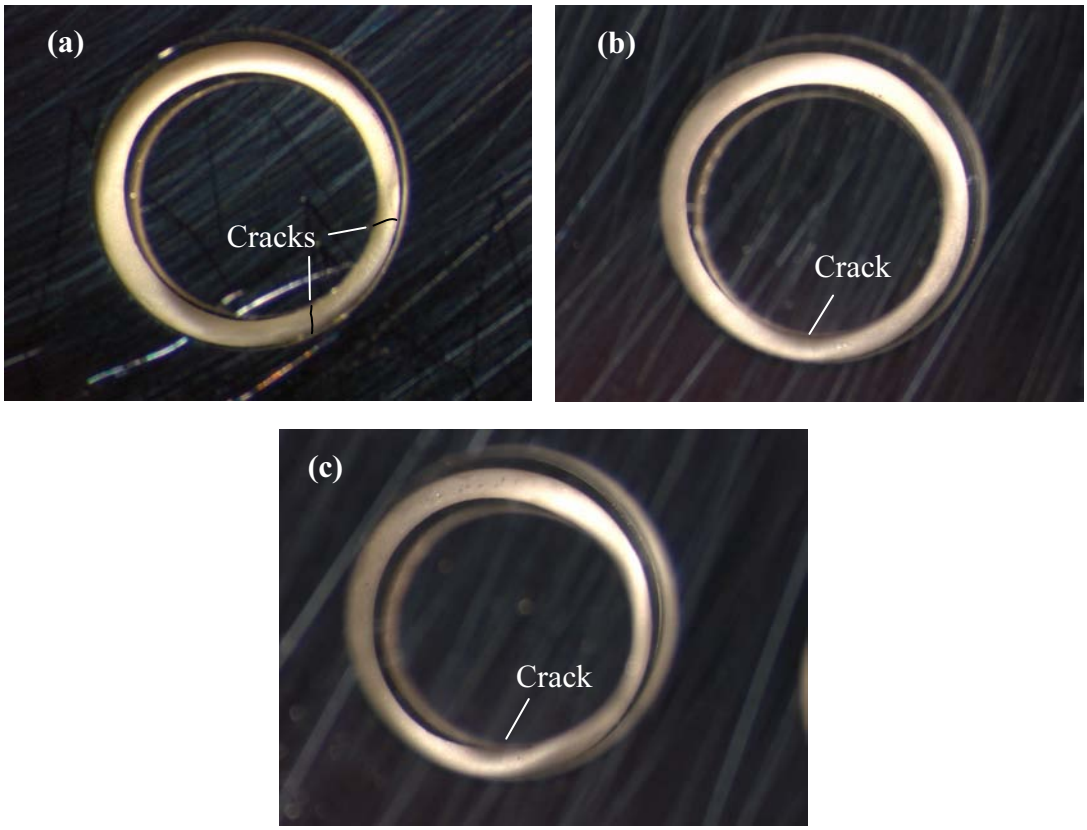

Fig. 17 Cracks in sleeves (a) A, (b) E, and (c) F. The cracks in Sleeve A are highlighted. The diameter of the web hole is approximately 2.32 mm.

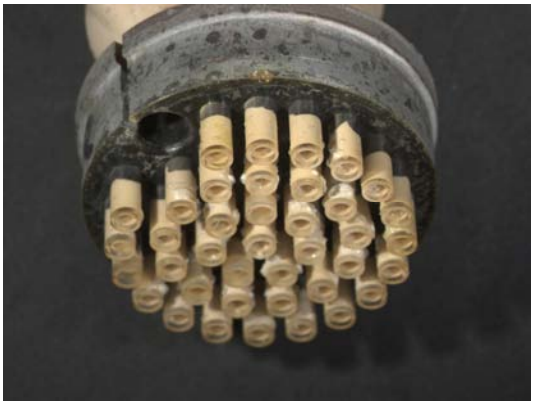

Fig. 18 Representative image showing rutile sleeves protruding from the amicon as well as the degree in which amicon wicked up the rutile sleeves (LAC SN102178-D81). Sleeve outside diameters are ~2.25 mm.

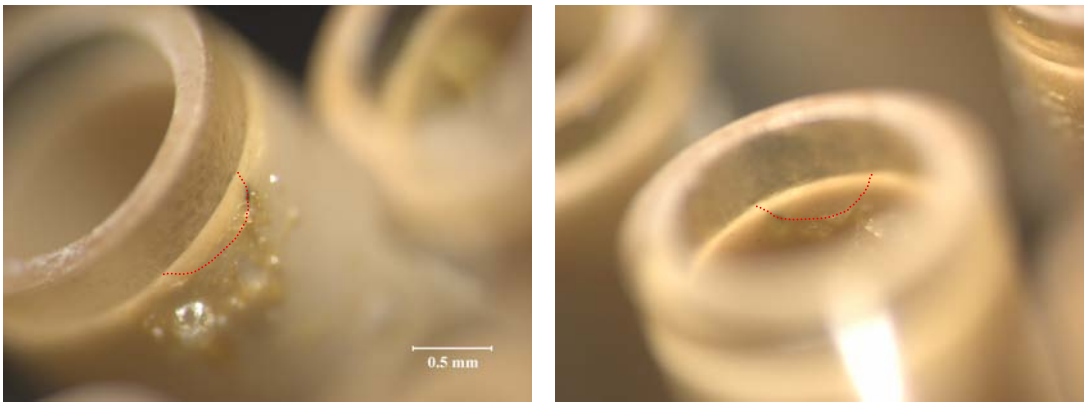

Fig. 19 Images outlining the trajectory of a crack in Sleeve A.

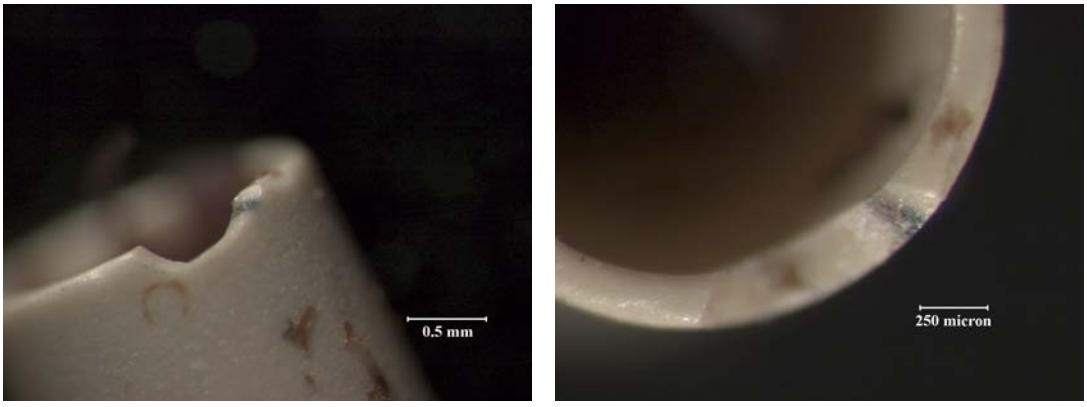

Fig. 20 During epoxy dissolution, the cracked portion of the sleeve fractured along the plane of a black mark. This black mark is evidence of a breakdown track.

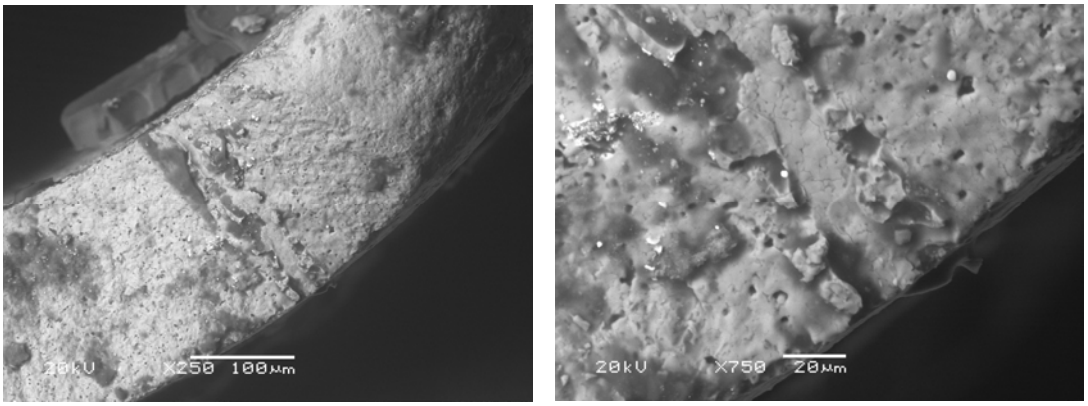

Fig. 21 SEM photomicrographs of the breakdown track in Sleeve A. Organic residue on the track surface is darker and should be ignored, it is an artifact of the air-chamber epoxy backfill and epoxy dissolution process.

ceramic. In the center of the black mark, a track extends through the thickness of the ceramic. The breakdown area has a fused character which is expected due to the high temperatures that are generated during a breakdown event. It appears the breakdown temperature was high enough to melt this portion of the rutile sleeve. The black track may be a thin layer of graphitic carbon or reduced titania on the surface.

Fortuitously, Sleeve W fractured (near the amicon base) during the epoxy dissolution process exposing a black mark on the crack surface (Fig. 22). As with Sleeve A, the black mark is evidence of high voltage breakdown occurring during the DCW test resulting in IR failures.

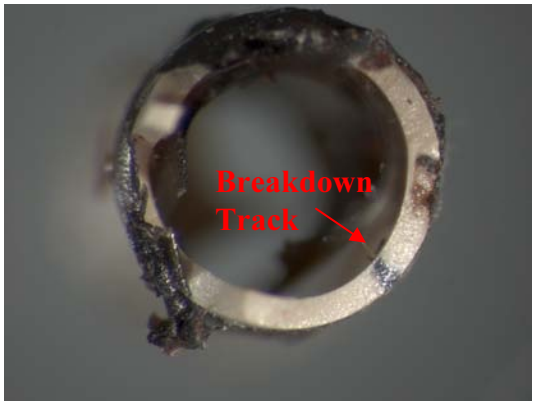

Fig. 22 Photomicrograph of a breakdown track in Sleeve W. Wall thickness of the rutile sleeves is approximately 225 µm.

5.3 LAC SN105251-K81

LAC SN105251-K81 broke down at 434 V after 1 sec. Subsequent IR at 510 V indicated that Pin B had a resistance of 1 Ω, thus failing IR requirements. Interestingly, Pin B had the lowest FRB of 898 V. All of the pin assemblies were asymmetrically aligned except

the Pin E assembly (Fig. 23). This pin passed FRB at 1725 V, which was the highest FRB of all the pins. The average was 1210 V. Most of the sleeves had small amounts of metallic contamination at their ends.

Sleeve B was isolated for additional characterization by carefully cutting around the Pin B assembly. During the cutting process, the sleeve fractured close to the amicon base. Along the fracture plane a black mark was observed (Fig. 24a). A similar mark, which is assumed to be a breakdown track, was also observed on sleeves A and W. However, Pins A and W did not register IR failures. SEM investigation of the black marks on Sleeves A, B (Fig. 24b), and W revealed the fused character associated with electric breakdowns. Fig. 25 illustrates the difference in microstructure of a breakdown area compared to the typical microstructure.

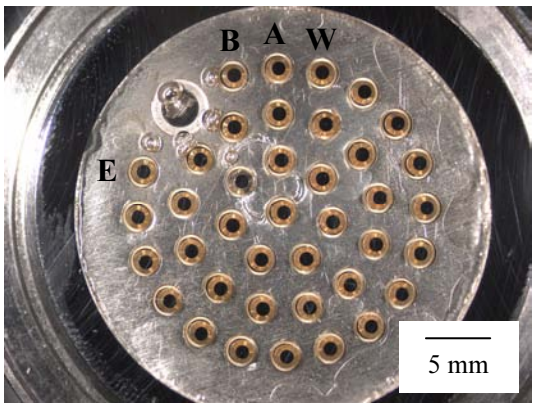

Fig. 23 Photomicrograph of LAC SN105251-K81 after the 1st polish. The Pin E assembly was symmetric with respect to the web, sleeve and pin resulting in the highest FRB of 1725 V.

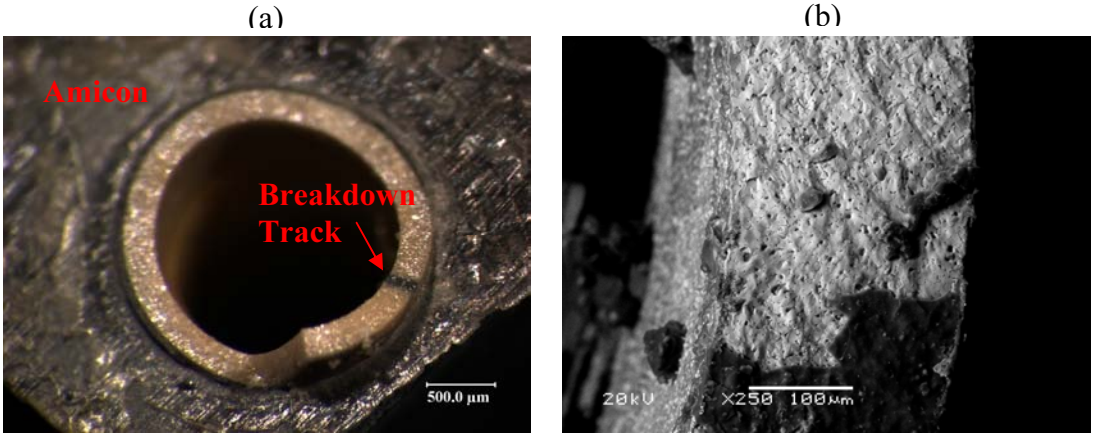

Fig. 24 (a) Optical photomicrograph illustrating the breakdown track on Sleeve B and (b) a SEM photomicrograph of the breakdown track in Sleeve B.

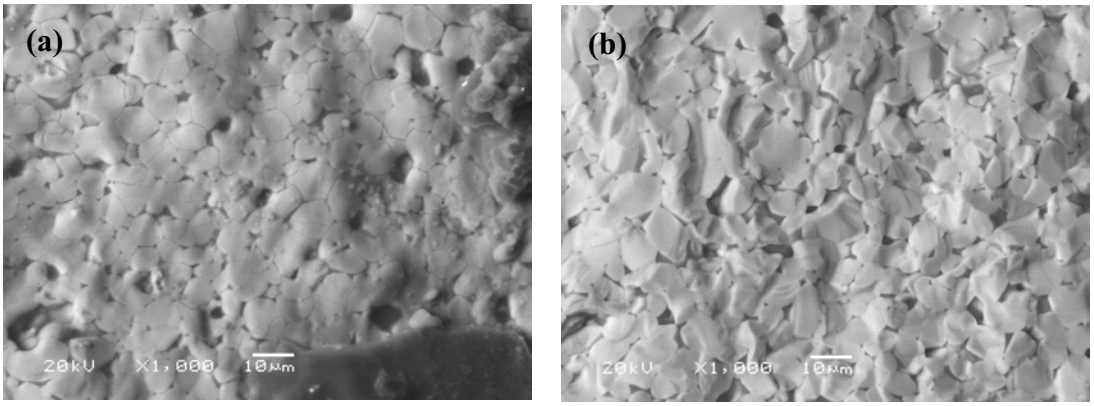

Fig. 25 SEM photomicrographs of the (a) breakdown track and of a (b) region away from the breakdown track in Sleeve B.

6. SUPPLEMENTAL CHARACTERIZATION

6.1 MICROSTRUCTURE

Porosity[5,6], grain size[5] and surface finish[7,8] have been shown to affect breakdown strengths of ceramic materials: as the amount of porosity and grain size increases the breakdown strength decreases. Similarly, it has been shown that ceramics with high surface roughness have lower breakdown strengths than ceramics that have a very fine surface finish. The surface finish relationship has been attributed to the material removal (grinding) process generating cracks which, depending on their severity, may act as the breakdown origin. Furthermore, the location of large grains, grain orientation, the size of pores, pore geometry and pore location may affect breakdown strengths. It has been shown that the dielectric strength of ceramic materials follow a Weibull distribution suggesting that failure-initiating flaws are randomly distributed throughout the ceramic.[7-9] Thus, a segment of the rutile sleeve population may breakdown at low strengths if it contains a failure-initiating flaw exhibiting the most severe conditions (the right location, size, shape, orientation for a low dielectric breakdown event).

Representative photomicrographs of polished cross-sections of rutile sleeves are shown in Fig. 26. All of the sleeves have a large amount of intergranular porosity. Qualitatively, all of the cross-sectioned sleeves have a wide range of pore size and geometry. Pore size and geometry appears slightly different for the sleeves in Figs. 26b &c compared to those in Figs. 26a,d,&e. The sleeves cross-sectioned and polished from LACs 902093-D79 and 105251-K81-1 appear to have a larger average grain size than the sleeves shown in Figs. 26a (LAC 805036-F78), d (105251-K81-2) and e (102178-D81). The difference in apparent grain size between LACs 105251-K81-1 and 105251-K81-2, underscores the fact that significant variations in microstructure should be expected even for sleeves used in the same LAC. With this variability in microstructure in mind as well as process variables (amicon height, sleeve wall thickness, sleeve surface finish, sleeve alignment and pin alignment), a large distribution in breakdown strengths would not be an unreasonable expectation.

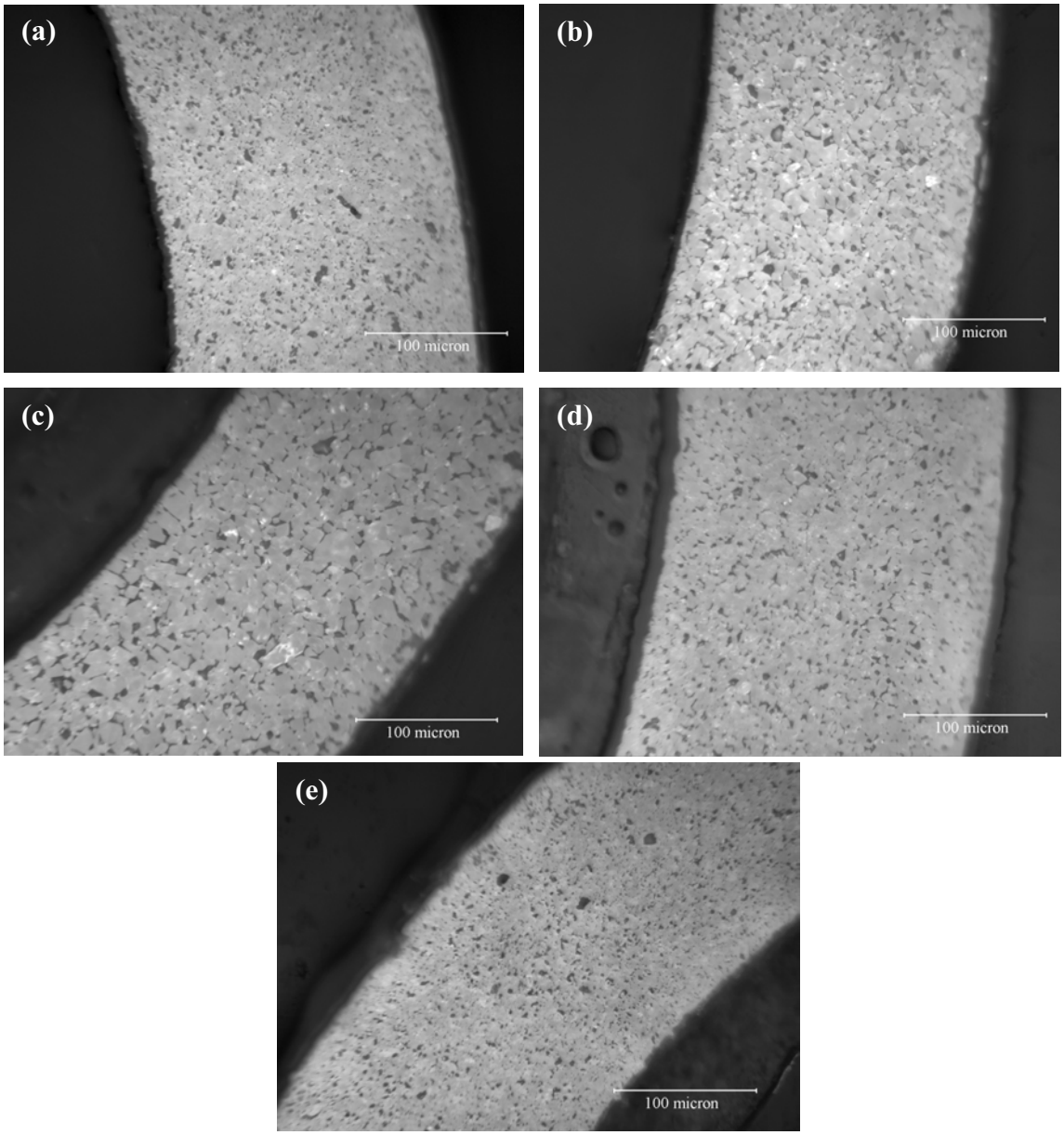

Fig. 26 Optical photomicrographs of cross-sectioned, mounted and polished rutile sleeves from LAC (a) 805036-F78, (b) 902093-D79, (c) 105251-K81-1, (d) 105251-K81-2 and (e) 102178-D81

6.2 HARDNESS AND FRACTURE TOUGHNESS

Sleeves from LACs 805036-F78, 902093-D79, 105251-K81 and 102178-D81 were mounted and polished for hardness and fracture toughness measurements. These measurements were performed to determine if material properties were consistent based on the date-code of each LAC. In addition, the measurements were made for comparison to published values. For the hardness and toughness measurements, a Vickers diamond indentor was loaded onto the optically polished surface for 15 s with a peak load of 4.9 N. Hardness was evaluated according to ASTM C1327-99. The indentation crack-length technique[10] was used to measure fracture toughness:

$$K_{Ic} = 0.016\left(\frac{E}{H}\right)^{\frac{1}{2}} \bullet \left(\frac{P}{c^{\frac{3}{2}}}\right) \quad (1)$$

where E is the modulus, P (N) is the indentation load, and $2c$ (mm) is the average length of the radial cracks emanating from the hardness impression . The modulus was assumed to be 192 GPa.[11] The hardness value incorporated in Eq. 1, defined as the peak indentation load divided by the projected contact area, is given by $H = 2P/d^2$ where d (mm) is the average length of the two diagonals. Vickers hardness and fracture toughness results are shown in Table 3 and Figs. 27 & 28. The Vickers hardness data are slightly lower than values obtain from the CenBASE Materials searchable database;[12] however, without knowing the density of the sleeves or the pedigree of the materials

Table 3. Vickers Hardness and Fracture Toughness Values of Rutile Sleeves

LAC Serial Number	Sleeve	Vickers Hardness (GPa)	Fracture Toughness (MPa·m$^{1/2}$)
805036-F78	1	7.62 ± 0.32	1.75 ± 0.31
805036-F78	2	7.38 ± 0.51	1.64 ± 0.27
902093-D79	1	7.26 ± 0.40	1.57 ± 0.16
102178-D81	1	7.81 ± 0.37	1.51 ± 0.16
105251-K81	1	7.14 ± 0.51	1.57 ± 0.22
105251-K81	2	7.37 ± 0.28	1.49 ± 0.22

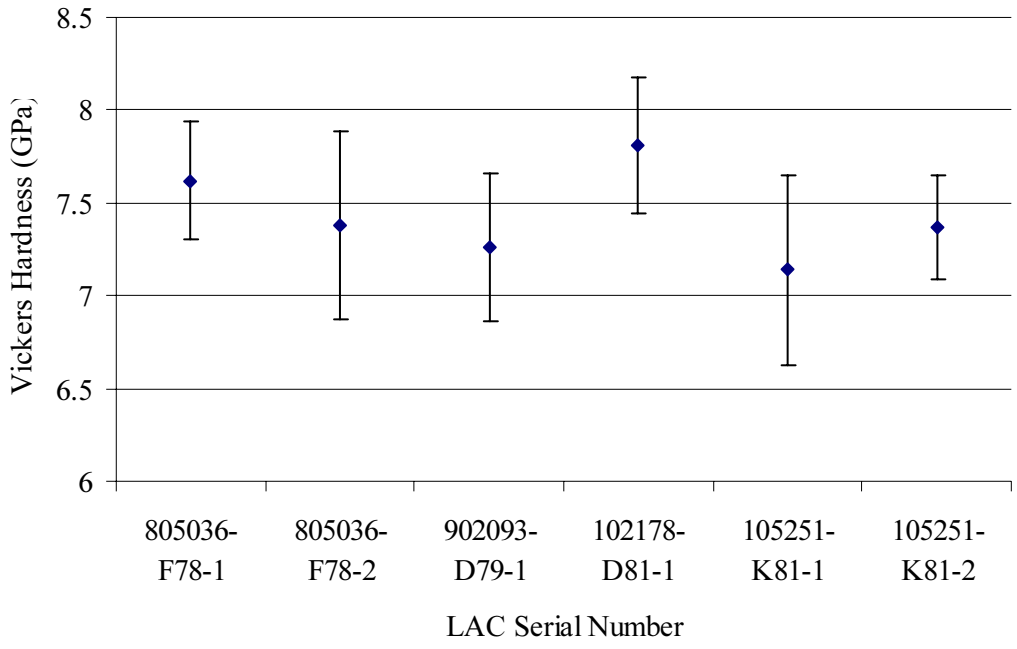

Fig. 27 Vickers hardness of rutile sleeves as a function of LAC serial number. The number at the end of each LAC serial number refers to the numbering convention used on the randomly selected sleeves.

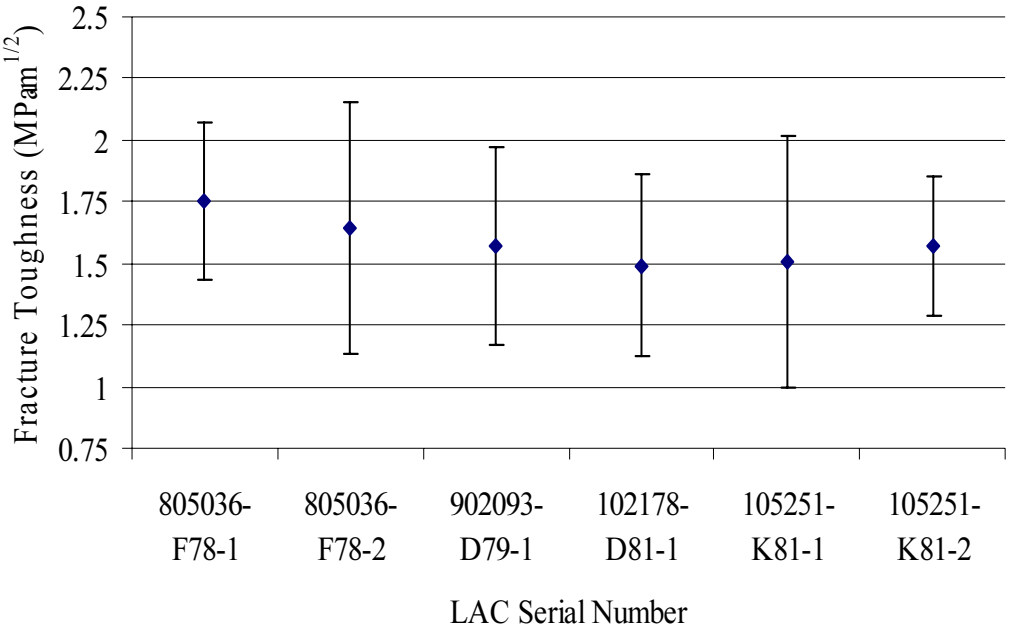

Fig. 28 Fracture toughness of rutile sleeves as a function of LAC serial number. The number at the end of each LAC serial number refers to the numbering convention of randomly selected sleeves.

listed in the database, direct comparisons to the published values cannot be made. Nonetheless, the hardness values (~7.4 GPa) are not drastically different than values obtained from the CenBASE Materials searchable database (~7.8 to 10 GPa). The average fracture toughness of rutile was calculated to be ~1.6 MPa·m$^{1/2}$ for all the sleeves tested. This value is partially based on of the assumed elastic modulus of 192 GPa (The assumed elastic modulus was the lowest published value.). A value of 2.2 MPa·m$^{1/2}$ was obtained from the CenBASE Materials searchable database. Because the value is based on manufacturers product catalogs where processing conditions of the rutile listed in the database are not known, direct comparisons cannot be made. However, the measured toughness values are not unusually low for a polycrystalline oxide ceramic. Also, there appears to be no systematic change in hardness (Fig. 27) and fracture toughness (Fig. 28) as a function of LAC fabrication date.

6.3 RAMAN SPECTROSCOPY AND SECONDARY ION MASS SPECTROMETRY

The black residue on the fracture surfaces associated with apparent breakdown events was examined with Raman Spectroscopy.[13] Raman was used to determine if the black residue was elemental carbon. This may be the case if carbon-containing species, for example from epoxy or hydrocarbons, infiltrated a defect which ultimately resulted in breakdown leaving a thin residual layer of elemental carbon. Raman spectra of the blackish region and the undamaged region showed similar patterns associated with rutile as well as an unidentified peak thought to be related to a vibrational overtone of rutile.[13] Patterns associated with elemental carbon were not evident. It was suggested that the black residue may be a thin layer of reduced titania. Rutile can be chemically reduced at temperatures as low 900°C. Reduced states of rutile are more conductive than stoichiometric rutile as well.[14]

Corollary to Raman, secondary ion mass spectrometry (SIMS) was used in an attempt to identify the content of the black residue.[15] Unfortunately, because of extensive surface contamination during the acid and epoxy dissolution process, SIMS was unable to identify the origin of the residual breakdown mark.

7. DISCUSSION

Porosity[5,6], grain size[5] and surface finish[7,8] have been shown to effect breakdown strengths of ceramic materials. Furthermore, the dielectric strength of ceramics is dependent on the testing methodology; for example, a ceramic that is exposed to voltages for sustained periods of time (seconds to minutes) will have a lower breakdown strength than the same ceramic that is pulsed with a high voltage which is more in the range of microseconds. In the case of the rutile sleeves, the distribution of porosity and grain size may result in premature breakdowns. Published breakdown strengths of rutile range between 20 kV/cm to 300 kV/cm.[7-9,16] The wide range in breakdown strengths is most likely due to differences in porosity, grain size, surface finish as well as experimental setup (volume of material tested, electrode configuration, voltage ramp rate, and time exposed to high fields).

The breakdown strength of the rutile used as the dielectric medium in the form of sleeves in LACs is not known. If we assume the dielectric strength is in the range of 20 kV/cm to 300 kV/cm, then there may be overlap between the testing criteria and the dielectric strengths of some sleeves. For instance, the DCW test requires a DC voltage of 510 V across the dielectric for 120 s. If we assume an average sleeve wall thickness of 225 μm, then the electric field across the rutile sleeve is 22.7 kV/cm. An electric field that is held across the dielectric for 120 s could induce a low voltage thermal breakdown in the ceramic due to Joule heating. For the FRB test, a high voltage pulse (10kV/μs) is applied across the ceramic where the expected breakdown path is near the rutile sleeve/air gap interface via gaseous surface discharge. The average dielectrically stimulated breakdowns by gaseous surface discharge in the air gap occurred at ~1250 V for the LACs that were examined as part of this study. Consequently, for a dielectrically stimulated breakdown to initiate in the air gap near the sleeve end, the ceramic must be able to withstand an electric field of ~56 kV/cm (assuming FRB occurred at 1250 V). For the sleeve to pass FRB requirements, a dielectrically stimulated breakdown in the air gap must occur at a voltage of 2000 V or less, thus the ceramic must be able to hold off an electric field of ~89 kV/cm. However, depending on the defect distribution in the sleeves (cracks, large pores, contact damage) and the alignment of the sleeve in the web slot, a sleeve could breakdown or begin to degrade during testing prior to a dielectric stimulated breakdown in the air gap near the end of the sleeve.

Cracked sleeves may also lower the dielectric strength of the ceramic. Through the sleeve extraction efforts, several of the sleeves were found to be cracked. The cracks were typically located in the sleeve that was in contact with the stainless steel webbing. Cracking may occur during assembly, while in the field or during the disassembly

process. The placement of the rutile sleeves in the slots within the stainless steel web could result in handling damage. If cracks were in the material prior to the amicon potting process, there is a potential for the amicon epoxy to seep into cracks, which could ultimately act as a failure initiation site. While in the field, a crack may initiate due to stresses associated with thermal cycling. Such a crack may be a weak link during subsequent testing. However, many of the sleeves examined in this study contained cracks but did not fail FRB/DCW/IR requirements. This may be because the crack was introduced during the disassembly process. If so, the crack was not present when testing was performed. Finite-element analysis (FEA) could be performed to estimate the magnitude of stresses in rutile sleeves that may have developed because of alignment issues and thermal cycling.

A definitive evaluation of the effect of porosity, grain size, surface finish and cracking on the breakdown strength of rutile sleeves cannot be made based on the failure analysis activities performed on the rutile sleeves in MC3080 LACs. To be able to link breakdown strength deviations to cracking and/or microstructural variations, a series of systematic experiments would need to be performed.[17] The intrinsic variability in the voltage required to initiate gaseous surface discharge (breakdown) in sleeve style LACs may also be from a source other than microstructural features: variations in dimensional tolerances (rutile sleeve thickness, rutile sleeve/pin alignment, sleeve surface finish and amicon height) could affect FRB. The source of FRB variation is further complicated by evidence showing that a sleeve that failed FRB on one test may pass FRB on subsequent tests or vice versa.[18]

8. SUMMARY

The failure analysis of rutile sleeves in MC3080 LACs was performed to determine the source of FRB/DCW/IR failures. The source of the FRB failure of Sleeve m in LAC SN902093-D79 may be associated with the combination of a smooth surface-finish, long-flow amicon, near-symmetrical alignment of the sleeve in the web slot and the slightly oversized inside diameter of the sleeve with respect to the pin. Similarly, Sleeve E from LAC SN105251-K81 which passed FRB (1745 V), but at the highest voltage of all the sleeves within this LAC, was found to be perfectly centered in the pin/web slot assembly. Specimens that failed DCW or IR requirements exhibit breakdown tracks. During a breakdown event within the ceramic, extensive localized melting and current localization destroys the breakdown origin, thus the source of IR/DCW failures in the examined LACs could not be determined. However, porosity or cracks in the ceramic could result in the lower breakdown strengths and ultimately IR/DCW failures.

9. REFERENCES

[1] T.L. Ernest, "Additional Information on the W80/B61 Lightning Arrestor Connector Significant Finding Notification," *Internal Memorandum to Distribution*, Sandia National Laboratories, Albuquerque, New Mexico, April 4, 2003.

[2] G.W. Franti, "Procedure for Performing Defect Analysis on Sleeve Style Lightning Arrestor Connecters (LACs)," *Laboratory Test Method 3281E*, Kansas City Plant, Kansas City, Missouri, November 11, 2000.

[3] W.E. Boyles, "Lightning Protection of Weapons Including Lightning Arrestor Connectors and Strong Link Switches," *Sandia National Laboratories Report*, SAND82-1181 (1983).

[4] R.A. Busefink, "Section Connector to Determine Cause of Fast Rise Failures," *Defect Analysis Report 883-0181*, Pinellas Plant, Largo, Florida, October 4, 1978.

[5] E.K. Beauchamp, "Effect of Microstructure on Pulse Electrical Strength of MgO," *Journal of the American Ceramic Society*, **54** [10] 484-87 (1971).

[6] A. Kishimoto, K. Koumoto, H. Yanagida and M. Nameki, "Microstructure Dependence of Mechanical and Dielectric Strengths – I. Porosity," *Engineering Fracture Mechanics*, **40** [4,5] 927-930 (1991).

[7] A. Kishimoto, K. Koumoto and H. Yanagida, "Comparison of Mechanical and Dielectric Strength Distributions for Variously Surface-Finished Titanium Dioxide Ceramics," *Journal of the American Ceramic Society*, **72** [8] 1373-76 (1989).

[8] A. Kishimoto and T. Tanaka, "High-Voltage Screening of Unidirectionally Surface-Ground Ceramics," *Journal of the American Ceramic Society*, **83** [6] 1413-16 (2000).

[9] K. Yamashita, K. Koumoto, M. Takata and H. Yanagida, "Analogy between Dielectric and Mechanical Strength Distributions of $BaTiO_3$ Ceramics," *Journal of the American Ceramic Society*, **67** [2] C31-C33 (1984).

[10] G. R. Anstis, P. Chantikul, B. R. Lawn, and D. B. Marshall, "A Critical-Evaluation of Indentation Techniques for Measuring Fracture-Toughness: I, Direct Crack Measurements," *Journal of the American Ceramic Society,* **64** [9], 533-538 (1981).

[11] R. G. Munro, *Elastic Moduli Data for Polycrystalline Ceramics*, NISTIR 6853, (2002), National Institute of Standards and Technology, Gaithersburg, Maryland 20899.

[12] CenBASE Materials Searchable Database, http://www.ran.sandia.gov/mat/, July 2, 2004.

[13] R.L. Simpson and D.R. Tallant, *Analysis Report: Job Number RAM04009*, Sandia National Laboratories, December 1, 2003.

[14] A.J. Moulson and J.M. Herbert, *Electroceramics: Materials, Properties and Applications*, Chapman & Hall, London, 1990, pp. 226-230.

[15] J.A. Ohlhausen, *Analysis Report: Job Number SIMS04012*, Sandia National Laboratories, August 2, 2004.

[16] D.W. Richerson, *Modern Ceramic Engineering*: *Properties, Processing, and Use in Design*, 2nd ed. Marcel Dekker, New York, p. 259.

[17] R. Tandon, B. Tuttle, C. Watson, and S. Monroe, "Proposals for Further Evaluation of Rutile Sleeves in B61 LACs," *Internal Memorandum to Terry Ernest (01733)*, Sandia National Laboratories, Albuquerque, New Mexico, June 15, 2004.

[18] T. Ernest, unpublished data.

EXTERNAL DISTRIBUTION

1	MS MF39	S. Marten, FM&T/KCP, D/EE1
1	MF39	B. Penniston, FM&T/KCP, D/EE1
1	SC4	G. Franti, FM&T/KCP, D/836
1	2C43	B. Gregg, FM&T/KCP, D/836
1	2C43	W. Tuohig, FM&T/KCP, D/836
1	2D39	E. Belarde, FM&T/KCP, D/EE1
1	2D39	D. Hasam, FM&T/KCP, D/EE1
1	2D39	C. Lula, FM&T/KCP, D/EE1

INTERNAL DISTRIBUTION

1	MS 0427	S.L. Hingorani, 02134
1	MS 0447	P.D. Hoover, 02111
1	MS 0523	L.A. Andrews, 01733
1	MS 0523	W.D. Cain, 01733
1	MS 0523	J.E. Christensen, 01733
1	MS 0523	T.L. Ernest, 01733
1	MS 0523	F.M. McCrory, 01733
1	MS 0885	G.E. Pike, 01801
1	MS 0886	R.P. Goehner, 01822
1	MS 0886	R.P. Grant, 01822
1	MS 0886	A.C. Kilgo, 01822
1	MS 0886	J.A. Ohlhausen, 01822
1	MS 0886	D.F. Susan, 01861
1	MS 0886	J.A. Van Den Avyle, 01822
1	MS 0888	R.A. Anderson, 01811
1	MS 0889	J.W. Braithwaite, 01861
1	MS 0889	J.S. Custer, 01851
1	MS 0889	S.J. Glass, 01851
1	MS 0889	S.L. Monroe, 01861
1	MS 0889	C. Newton, 01851
1	MS 0889	C.J. Roth, 01851
1	MS 0889	R. Tandon, 01851
1	MS 0959	C.B. Diantonio, 14154
1	MS 0959	T.J. Gardner, 14154
1	MS 0959	S.J. Lockwood, 14154
1	MS 0959	R.H. Moore, 14154
1	MS 0959	R.G. Stone, 14154
5	MS 0959	C.S. Watson, 14154
1	MS 0959	P. Yang, 14154
1	MS 0961	C. Adkins, 14150
1	MS 1349	W.F. Hammetter, 01843
1	MS 1411	R.L. Simpson, 01822

1	MS 1411	D.R. Tallant, 01822
1	MS 1411	W.R. Olson, 01851
1	MS 1411	B.A. Tuttle, 01851
2	MS 9018	Central Technical Files, 8945-1
2	MS 0899	Technical Library, 4536